SOIL SCIENCE ANNUAL
2025, 76(3), 208825

https://doi.org/10.37501/soilsa/208825

A case study of the temporal stability of soil electrical conductivity for a sandy field and the usefulness of its measurement for the preparation of agronomic category maps

Stanisław Marek Samborski[1*], Michał Stępień[1,2], Yunus Emre Şekerli[3]

[1] Warsaw University of Life Sciences – SGGW, Institute of Agriculture, Department of Agronomy, 02-776 Warsaw, Poland
[2] Warsaw University of Life Sciences – SGGW, Institute of Agriculture, Department of Biometry, 02-776 Warsaw, Poland
[3] Hatay Mustafa Kemal University, Faculty of Agriculture, Department of Biosystems Engineering, 31040 Antakya, Hatay, Türkiye

* Corresponding author: Dr hab. Stanisław Marek Samborski, stanislaw_samborski@sggw.edu.pl, ORCID iD: https://orcid.org/0000-0003-1147-5805

Received: 2025-02-14
Accepted: 2025-07-31
Published online: 2025-07-31
Associated editor: Cezary Kabała

Keywords:

Soil texture
Agronomic category
Light and light soils
Apparent electrical conductivity
Temporal stability

Abstract

One of the most commonly used sensing technologies to characterize soil spatial variability is on-the-go measurement of the apparent electrical conductivity (EC_a). When properly calibrated to conventional soil properties, EC_a measurements can help to create thematic soil maps that represent the variability of soil characteristics. Then, these maps, after reclassification, can be used for the creation of prescription maps for variable application of agricultural inputs, to increase their use efficiency. In the absence of salinity, EC_a is strongly responsive to soil texture (ST), which is more stable over time than chemical soil properties. However, the temporal stability of soil EC_a on commercial fields has not been investigated in Poland, which has a wide representation of very light and light soils. In our country, four soil agronomic categories (ACs) were distinguished, and they are derived from information on the content of fine particles (FPs, <0.02 mm) in the soil. ACs have been used for the formulation of lime and fertilizer recommendations in our country and they are typically assigned through laboratory determinations of fine particle content or derived from soil agricultural maps. But, none of these approaches allows for the delineation of soil ACs with high spatial density required for the creation of maps for variable application of agricultural inputs. The objectives of the study were to: i) evaluate spatial and temporal variability of relative EC_a values registered at two depths (EC_{sh} – 0–30 and EC_{dp} – 0–90 cm), during eight EC_a surveys for a commercial field of predominantly very light and light soils; ii) delineate soil ACs for this field based on the relationship between EC_a values registered during two surveys done in a 10-year time interval, and fine particle content. The production field was characterized by high EC_a spatial variability and stable temporal EC_a patterns, suggesting that a single measurement of this soil property could be sufficient to delineate maps of soil physical characteristics strongly related to EC_a on very light and light soils. A strong relationship between the relative EC_{sh} values from 2013 and 2023, and fine soil particles allowed the creation of very similar maps of ACs, which may be used for formulating fertilizer and lime recommendations on fields covered with the above-mentioned types of soils. The soil ACs patterns were less repeatable across years (2013 vs. 2023), but acceptable for map generalization when the EC_{dp} values were used for the prediction of FPs content from a thicker soil layer (0–90 cm). However, the wider application of achieved relationships may require field-specific calibrations of EC_a values to ensure better accuracy of the delineated AC maps because this study was performed in a single production field.

1. Introduction

Soil properties vary considerably over most fields, often leading to variable crop production (GRDC 2023). Thus, the information about the spatial variability of different soil attributes within a field is essential for the decision-making process (Adamchuk et al., 2004), which is done by the farmers mainly through the more efficient use of inputs (nutrients, ameliorants, pesticides, and water). Proximal soil sensing (PSS) involves on-the-go (while travelling across the field) collection

Supplementary materials are available at: https://www.soilsa.com/SuppFile/208825/1/

of information related to soil properties, often employing one or more sensors. These sensors are integrated with positioning information from global navigation satellite systems (GNSS), that allow to produce geo-referenced maps showing variation across the surveyed area (GRDC 2023). The PSS sensing systems are based on diverse real-time or near real-time measurement concepts, including electrical and electromagnetic, optical and radiometric, mechanistic, and electrochemical (McKenzie et al., 2003; Adamchuk et al., 2004). Recently, the Grains Research and Development Corporation – GRDC (2023), published an overview describing the advantages and disadvantages of different PSS available to farmers and summarized that among the commercially available PSS on-the-go systems are: electromagnetic induction (EMI) or electrical resistivity measurement, both used to determine soil electrical conductivity (EC), gamma-radiometer (passive), ion-selective electrode, visible/near infrared spectrometry (active). However, despite this great variety of design concepts, most PSS being developed rely on measuring the soil's ability to reflect or emit electromagnetic energy or quantify the amount of electrical charge that soil media can conduct and/or accumulate (Adamchuk et al., 2011). Moreover, georeferenced EC_a measurements are well suited for characterizing the spatial distribution of soil properties because they are reliable, quick, and easy to take with commercial equipment (Corwin and Scudiero, 2020). In agriculture, soil spatial variability has been characterized by the use of the apparent electrical (EC_a) conductivity for more than two decades (Corwin and Lesch, 2003). There are two main methods applied to measure soil EC_a. A non-contact EMI and a contact method which uses rotating metal discs as electrodes, which penetrate the soil surface (Farahani and Buchleiter, 2004). The latter method does not need calibration and the EC_a measurements are not affected by power lines or nearby metal objects buried in the soil.

No single EMI survey or the relative difference in EC_a of repeated EMI surveys was sufficient to obtain the best possible soil map for the study area (Zhu et al., 2010). The more EC_a surveys carried out in a given area, the more information collected about the spatial variation of soil properties (Pedrera-Parrilla et al., 2016). However, such an approach seems only reasonable if at least some other soil characteristics affecting EC_a readings are also determined at the time of these measurements, to calibrate EC_a measurements to conventional soil properties. Costly and time-consuming procedures of soil analyses very often limit such extensive studies and are not cost-effective beyond research activities. Nevertheless, information from several EC_a surveys is important because it allows for checking if a particular soil under such a cropping system and climatic conditions shows temporal stability of EC_a values, i.e. similar EC_a patterns across the years. If delineated EC_a zones are to be used to manage agricultural inputs across the field for multiple years, the spatial variability and temporal stability of this soil property is of significant importance (Farahani and Buchleiter, 2004). In the absence of salinity a dynamic property, research results show that soil EC_a, frequently responds well to soil texture (ST), which is more stable over time than chemical soil properties (Corwin and Scudiero, 2020). EC_a is also a qualitative indicator in areas with high spatial variability in ST (Molin and Faulin, 2013). Research indicates that EC_a is influenced by various soil characteristics, including clay content and moisture levels, which can vary significantly over time and location (Molin and Faulin, 2013; Bottega et al., 2017; Atwell and Wuddivira, 2019). In Poland, four groupings of ST classes called soil agronomic categories (ACs), namely very light, light, medium and heavy, have been used since 1986 for formulating lime and fertilizer recommendations (Zalecenia nawozowe, 1990; Jadczyszyn et al., 2010; Jadczyszyn et al., 2016) and are also one of the main criteria used to delineate land suitability groups (In Polish: "kompleks przydatności rolniczej gleby" Witek, 1973). These land suitability groups or frequently also the ACs, determined to a depth of about 1 m, could be called "management zones" (MZ) or zone boundaries which according to Adamchuk et al. (2021), have distinct water and nutrient storage potential and could be linked to changes in some chemical properties caused by natural processes under uniform field management. So far, the ACs are assigned to soils by laboratory determination of the amount of fine particles (FPs, <0.02 mm) in the soil or are derived from soil agricultural maps (Stępień et al., 2024b). Thus none of these approaches allows for the delineation of soil ACs with high spatial density required for variable application of agricultural inputs according to locally defined needs to increase their use efficiency (Pierce and Nowak, 1999; Stępień and Samborski, 2018). However, earlier findings show a strong relationship between soil separates and EC_a measured with the non-contact EMI (Stępień et al., 2015) and contact EC_a method (Stępień et al., 2017) used in Poland. The stability of field-scale EC_a measured with the contact method over a few years on fields exposed to different cultural and cropping practices has not been examined in Poland, which has a wide representation of very light (mainly sands according to USDA, 28% of the area of agricultural land) and light (mainly loamy sands and some sandy loams, 30%) soils (Łopatka, 2017). A higher stability of EC_a for soils with higher sand contents due to the lower interactions of EC_a with water content and soil chemical properties in such soils compared with clay soils was suggested by Ahrends et al., (2023).

The objectives of this study were to: i) evaluate spatial and temporal variability of relative soil shallow (EC_{sh}) and deep (EC_{dp}) measurements registered during eight EC_a surveys for a production field of predominantly very light and light ST; ii) determine soil ACs for this field based on the relationship between soil EC_{sh} and EC_{dp} values, measured during two surveys done in a 10-year time interval, and FP content.

2. Materials and methods

2.1. Location of the research area and weather conditions

The study was conducted between 2013 and 2023 on a production field of 10.5 ha (Fig. 1), located in Obory, in Mazovia region of Poland (52°4'54"N, 21°8'32"E), situated in the Central Poland Lowland, code 318 (Solon et al., 2018). This region occupies about 27% of the area of Poland (Richling et al., 2021) and belongs to the Central European Lowland. The field is located in

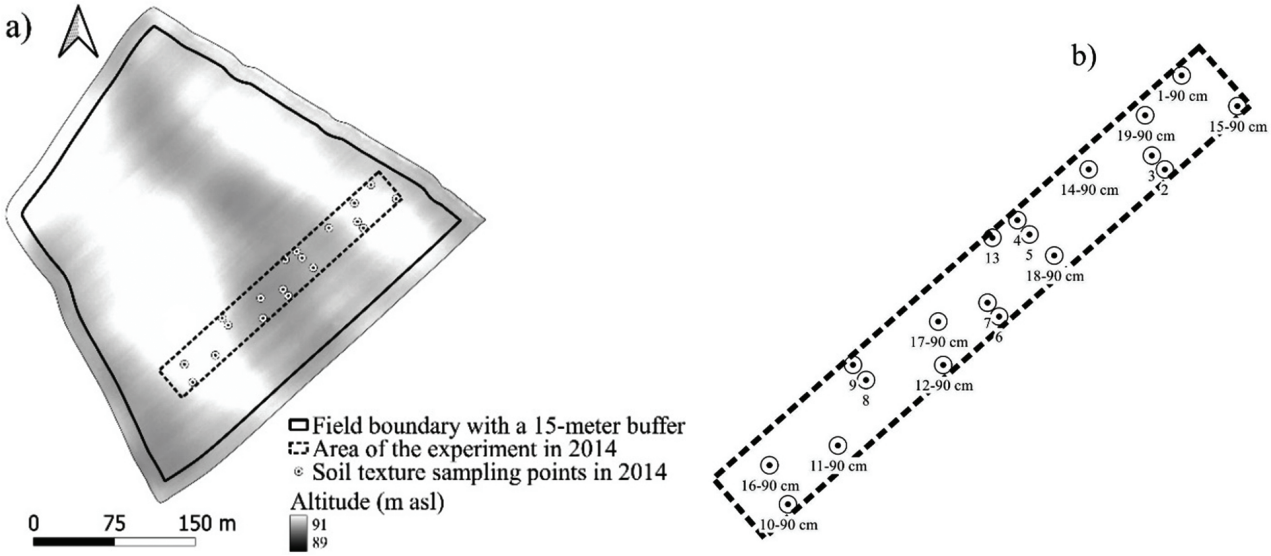

Fig. 1. Maps of the: a) field with a superimposed area (0.90 ha) of an experiment, soil texture sampling points in 2014, and altitude (m) model (source: https://www.geoportal.gov.pl); b) distribution of the soil sampling points within the experimental area. Points only with numbers refer to areas where samples were taken from a depth of 0–30 cm; points with a label of 90 cm, refer to areas where samples were taken to a depth of 90 cm

a former valley floor on the toeslope of the escarpment and has a flat to gently undulated surface, with an altitude in the range of 89–91 m (Stępień et al., 2015). The soils of this field are formed mainly from fluvial sands, gravels, and alluvial sediments, according to the Detailed Geological Map of Poland (Sarnacka, 1976). The field is covered mainly by Arenosols (AR) and Luvisols (LV) according to WRB (IUSS Working Group WRB, 2022) and rusty soils (BV), clay-illuvial soils (PP) and arenosols (SN) according to the 6th edition of Polish Soil Classification (Kabała et al. 2019; Systematyka Gleb Polski, 2019). The main ST classes found in this field are sand and loamy sand, although some areas of sandy loam are also present in the topsoil (Stępień et al., 2015). Finer textured soils, namely sandy clay loams and clay loams were found in some layers of the subsoil in some of the field areas (Bioprodukty, 2013–15).

Weather data were acquired from the Warsaw-Okęcie weather station located approximately 13 km from the study field (https://danepubliczne.imgw.pl). Mean annual precipitation and air temperature varied from 390 mm to 705 mm and from 8.91°C to 10.9°C, respectively, at the time of this study (Table 1s and 2s, supplementary materials).

2.2. Management of the field and measurements of absolute EC values

The basic information on the field management during the study period of 2013–2023 is presented in table 1. At this time all field operations and all production inputs were applied uniformly across the field. Measurements of EC (mS m^{-1}), were taken using on-the-go Veris Mobile Sensor Platform – MSP3 (Veris Technologies, Inc., Salina, Kansas, USA), mounted on an agricultural tractor. The Veris is equipped with six coulter electrodes mounted on an implement. One pair (emitters) of the coulters induces an electrical current in the soil, while the other two pairs of coulters (receivers) positioned at distances of 0.3 and 0.9 m from the inducing electrodes, measure the voltage drop simultaneously. This voltage drop is expressed as EC_a at two depths: shallow (0–0.30 m) – EC_{sh}, and deep (0 to 0.90 m) – EC_{dp}, respectively, at a 1 Hz logging rate. The electrodes are inserted a few centimeters into the soil to ensure their direct contact with this medium. Field-scale EC mappings were conducted in the fall after harvest and shallow tillage, with two exceptions. Namely, in 2013, the EC_a measurements were done five weeks after sowing winter wheat, and in 2019 the EC_a survey was done in the spring (Table 1). To avoid the influence of more compacted areas (tramlines) on the EC_a readings, in all years the EC_a measurements were performed at a slight angle towards the tramlines used during the cultivation of the previous or existing (in 2013) crops. On average, travel speeds through the field ranged between 7.2 and 10.8 km h^{-1} with measurements taken every second, corresponding to 2 to 3 m spacing between measurements in the direction of travel, respectively. The EC_a measurements were tagged with position information provided by a GNSS unit (Garmin 19x, Garmin International Inc., Olathe, Kansas, USA). To guide parallel passes through the field at 7.5 m or 15 m (only in 2013 and 2019), an Integra display connected to another GNSS receiver – GPS 1600 (Ag Leader Technology, Ames, Iowa, USA), mounted on the tractor's roof was used.

2.3. Soil texture determination

The ST data come from a part of the field (~0.90 ha, Fig. 1), where an experiment was conducted in 2014, to test the effect of nitrogen and sulfur fertilization on yield, quality, and nitrogen use efficiency of winter wheat. Soil sampling was performed on two dates: March, 2014 (ten soil augerings to a depth of 30 cm, four of the ten to a depth of 90 cm) and August, 2014 (four soil profiles to a depth of 100 cm and five additional soil augerings to

Table 1
Basic management information regarding conditions of the EC measurements: dates, previous crop, field status at the time of the EC surveys

EC survey date	Previous crop	Field status at the time of EC measurement or tillage equipment used 2–4 weeks before the EC survey*
18.11.2013	Winter rape *Brassica napus* L.	Growing winter wheat, BBCH 22–23
07.11.2014	Winter wheat *Triticum aestivum* L.	FYM (30 t·ha^{-1}) mixed with soil using a spading harrow of Duro France Compil COM 710 (7 m*)
23.10.2015	Corn *Zea mays* L.	Stubble
04.11.2016	Potato *Solanum tuberosum* L.	Post-harvest field
13.10.2017	Winter wheat *Triticum aestivum* L.	Disk harrow of Lemken Rubin 9/450 KUA (4.5 m)
19.10.2018	Corn for silage *Zea mays* L.	Cultivator Amazone Cenius 3002 (3 m)
30.03.2019	Corn for silage *Zea mays* L.	Tillage unit of KLEIN U 429/3 (3.6 m)
27.10.2023	Winter rape *Brassica napus* L.	Spading harrow of Duro France Compil COM 710 (7 m)

* – in brackets, working width of the machinery,

a depth of 90 cm, but one of the samples to a depth of 90 cm was missing). The soil samples from all kinds of samplings were air-dried, sieved by a 2 mm diameter mesh size, and analyzed for the particle size distribution using the sieve-hydrometric method of Bouyoucos modified by Casagrande and Prószyński (Stępień et al., 2024a, 2024b). Then, the soil samples were classified according to the most updated ST classification used in Poland – PTG 2008 (referred to as PTG 2008/USDA) – and BN 1978 which was a base for the definition of ACs (Stępień et al., 2024a, 2024b). As the soil horizons had different thicknesses, the weighted average values of the contents of soil separates for layers 0–30 cm and 0–90 cm were calculated, based on 19 and 10 soil samples, respectively.

2.4. Transformation of absolute EC_a values

In some years, a western part of the field, located close to the escarpment, was inaccessible because of wet spots, and thus, EC_a readings from this part of the field were missing. Moreover, three out of four edges of the field are affected by trees. Therefore, to avoid field edge effects (Corwin and Scudiero 2020), the whole field boundary was cropped by a 15-meter buffer zone, and as a result, the whole field investigated area was reduced to 8.63 ha (Fig. 1). EC_a data from each survey were interpolated using an ordinary kriging method supported by a plug-in *SmartMap*, version 1.4.2 installed in QGIS.org. Spherical semivariograms were fitted to both EC_{sh} and EC_{dp} for each EC survey as recommended by Bohling (2005), because spherical models exhibit linear behavior at the origin and are appropriate for representing properties with a higher level of short-range variability. To ensure the same number of the same points for each year, the interpolation grid size, to which an average EC_{sh} or EC_{dp} value was assigned, was set to 10 m x 10 m. The total number of points for each year was 863. In order to extract the pixel values from the raster layers of EC_{sh} and EC_{dp} from 2013, at the nineteenth ST sampling points, the *sample raster values* functionality available in QGIS was used.

2.5. Descriptive statistics and regression analysis

The mean, minimum, maximum, standard deviation (Std), and percent of coefficient of variance (CV) were calculated for raw (non-interpolated) and interpolated EC data. The whole set of EC_{dp} data collected in November 2014 included a significant number of spurious (negative) values. Therefore, these data were not used in further analyses. The possible explanations for such a phenomenon could be the spreading of farmyard manure and mixing with very dry soil soon before the EC survey in 2014 (Table 1). We supposed that in such conditions, the coulters penetration was deteriorated, resulting in loss of physical contact between the coulter electrodes and soil, which caused the registration of the negative EC_{dp} values. A close contact between the electrodes and soil can only be attained when the soil surface is moist (Corwin and Scudiero, 2020).

The same number of points for the interpolated EC_{sh} and EC_{dp} data for each year, allowed us to perform regression analysis of the relathionship between the EC data registered at different dates and calculate the Pearson correlation coefficients (r) using Microsoft® Excel (Microsoft Corporation, Redmond, Washington, United States).

2.6. Normalization of the absolute EC values

To overcome the effect of different soil conditions (soil moisture, field status), during EC_a surveys, the values of the interpolated EC_{sh} and EC_{dp} were divided by the average value of EC_{sh} and EC_{dp} of the whole-field set of EC data, respectively. This approach to EC_a data normalization was applied by Serrano et al., (2017), and it allows very simple calculation and interpretation. The purpose of this procedure was to transform the absolute EC_{sh} and EC_{dp} values into relative values. The sets of relative EC_{sh} and EC_{dp} values from each EC_a survey were divided into three classes: 0–1, 1–2, and 2–3. Relative EC_a values equal to 1 or below one mean that the absolute EC_a value equaled the whole-field average EC_a or was below this value. Normalized EC_{sh} and EC_{dp} values in the ranges from 1 to 2 and from 2 to 3 mean that the absolute EC_a value was from 1 to 2, and from 2 to 3 times higher than the whole-field average EC_a, respectively. Using the same three classes of relative EC_{sh} and EC_{dp} values, made visually comparing the spatial EC_a variability within years easier. Different approaches to EC_a data normalization have been used in the scientific literature. For example, Serrano et al., (2017) used the average value of EC_a of the whole set of data, Farahani and Buchleiter (2004) applied EC_{index}; Badewa et al., (2019) used the standard deviation of the relative differences. Recently, Gonçalves et al. (2025) compared three methods of EC_a data normalization, namely – range, average, and standard score.

2.7. Principal component analysis and time series analysis of the EC_a values

To identify which particle size fraction has the greatest impact on EC_a values the principal component analysis (PCA) was performed using StatSoft, Inc. STATISTICA (data analysis software system), version 13. www.statsoft.com.

Time series analysis was used to identify long-term changes in EC_a values for the same areas of the field within years. For this purpose, an analysis of regression was performed in Microsoft® Excel, where EC_a was treated as the dependent variable, and years of EC_a measurements as the independent variable. The slope value of the regression line was used to describe the rate of change in the dependent variable for a one-unit change in the independent variable.

2.8. Temporal stability analysis and creation of ACs maps

This analysis of the relative EC_a data was determined by calculating the coefficient of variance for each of the 863 points over the eight (EC_{sh}) and seven (EC_{dp}) years of evaluation (Blackmore, 2000). The CV was classified according to Gonçalves et al. (2025), who used the classification of CV into: low – CV ≤10%, medium – 10% < CV ≤ 20%, high – 20% < CV ≤30%, and very high – CV >30%, originally proposed by Pimentel-Gomes (2023).

The strength of the relationship between the relative EC_a values and the soil separates (sand, silt, clay according to PTG 2008/USDA and FPs according to BN 1978) was evaluated using the determination coefficient (R^2) of the best-fitted equation. Mean absolute error (MAE), was used to measure the prediction error of FPs content using the relative values of EC_a and the best-fitted regression model.

$$MAE = \frac{\sum_{i=1}^{n} |y_{i-} x_i|}{n}$$

where y_i was the predicted FPs content and x_i was the true (measured) value of FPs content.

Relative EC_{sh} and EC_{dp} values were used to create spatial maps of soil ACs based on predicted FPs content using the best-fitted equation. To derive the soil ACs, the following content of predicted FPs was used: below 10% – very light, between 10 and 20% – light, and between 20 and 35% – medium (Zalecenia nawozowe, 1990).

3. Results and discussion

3.1. The content of soil separates in soil layers of 0–30 and 0–90 cm, sampled in 2014

The soil of the area of the experiment was classified, on average, as loamy sand (PTG 2008/USDA) in the topsoil (0–30 cm) and the 0–90 cm layer and as strong loamy sand in the topsoil and light loamy sand (pgm and pgl, respectively, according to BN 1978 and PTG 1956 – ST classifications, Stępień et al., 2024b) in the thicker layer (Table 2). These data indicate that the same prevailing ST classes were found on this field (referred to as field C) during the previous soil studies conducted in 2009 (Stępień et al., 2015; Stępień et al., 2016), when the topsoil was sampled at 21 soil sampling points distributed evenly across the whole field area. This shows that the topsoil of the experimental area (~0.9 ha) in 2014 was representative of the entire field (8.63 ha). Based on this, we assumed that the laboratory-determined content of soil separates could be utilized to develop calibration models of the EC_a values using regression equations.

3.2. Variation of absolute raw EC_{sh} and EC_{dp} values within a field at subsequent EC surveys

During all eight EC surveys low and very low absolute EC values were registered (Table 3), which indicates coarse ST. The general range for EC_{sh} and EC_{dp} values registered across all years was from 0.39 to 15.9 mS m^{-1}, and from 0.01 to 13.3 mS m^{-1}, respectively. The ranges of the absolute EC_a values obtained at different dates also varied, as in many previous studies on multiple EC_a measurements, done using mainly EMI (Zhu et al., 2010; De Caires et al., 2014; Pedrera-Parrilla et al., 2016; Serrano et al., 2017; Gonçalves et al., 2025) but also with a contact method (Terrón et al., 2013; Nyéki et al., 2022). In the case of EC_a measurements at both depths, the highest average EC_a values were registered on March 30th of 2019 – during the only spring EC_a survey (Table 1), while the lowest were in 2013 for EC_{sh} and in 2023 for EC_{dp}. This may suggest higher soil moisture at the spring EC_a measurement than during the all autumn

Table 2
Descriptive statistics of soil separates in soil layers of 0–30 and 0–90 cm sampled in 2014

Soil layer (number of soil evaluation points)	Soil texture classification	Soil fraction (diameter)	The content of soil separates (%)				
			Min	Max	Mean (median)	Std	CV
0–30 cm (19)	PTG 2008/USDA	Sand 2.0–0.05 mm	64.0	91.0	76.4 (75.0)	7.7	10.0
		Silt 0.05–0.002 mm	6.0	26.0	17.5 (18.0)	6.2	35.5
		Clay <0.002 mm	3.0	11.0	6.1 (5.1)	2.5	40.8
	PTG 1956	Sand 1.0–0.1 mm	55.8	85.5	67.6 (67.0)	9.1	13.4
		Silt 0.1–0.02 mm	7.0	23.1	16.2 (17.0)	4.7	28.9
		Fine particles (<0.02 mm)	6.0	22.1	16.2 (17.1)	4.9	30.7
0–90 cm (10)*	PTG 2008/USDA	Sand 2.0–0.05 mm	66.0	94.0	80.2 (80.8)	11.0	13.7
		Silt 0.05–0.002 mm	4.2	22.0	12.7 (12.9)	6.9	54.4
		Clay <0.002 mm	1.7	14.6	7.1 (6.5)	4.7	65.9
	PTG 1956	Sand 1.0–0.1 mm	56.9	90.1	72.5 (70.7)	13.0	18.0
		Silt 0.1–0.02 mm	5.2	21.7	13.4 (13.2)	6.0	44.9
		Fine particles (<0.02 mm)	4.7	24.7	14.2 (14.2)	7.7	54.3

* – for this layer, the weighted average values of soil separates from different layers were calculated

EC_a surveys. Nevertheless, at none of the eight soil EC surveys, soil moisture was registered, and the total amount of rainfall in March 2019 was only 27.9 mm in the nearest meteorological station in Warsaw-Okęcie (Table 1s, supplementary materials), but the soil could have accumulated some more water. This is because since the beginning of November 2018, the soil has not been disturbed by tillage, and the air temperature during the winter did not favor transpiration. Additionally, a fertilizer Super Kali (37% of K_2O, 7% of CaO, 3% of MgO, 21% of SO_3) was spread a month before the EC_a survey in March 2019, which could have elevated the soil solution concentration, thus increasing EC_{sh} and EC_{dp} values. A stronger effect of potassium fertilizer than phosphorus and nitrogen fertilizers on EC values in a laboratory and in field experiments was reported by Lueck (2015), and the effect of increasing doses of potassium fertilizers on soil EC_a was also observed by de Farias et al. (2018). In the other years of our research, the time gap between the application of fertilizers and EC_a surveys was much longer than in 2019. On average, the effect of the accumulated rainfall obtained in the month before the EC_a measurements seems to be very weak. This is because in the years when the precipitation in the above period was the highest, i.e., 2016, 2017, and 2018 (Table 1s, supplementary materials), the mean values of the EC_a measurements at both depths were not the highest but relatively low (Table 3). One of the explanations of this phenomenon is that the sandy soil of this field (Table 2), are characterized by low water holding capacity. Our EC_a measurements were done in conditions when the soil temperature did not change significantly. This is because these measurements took place in autumn and spring (2019), on days when cloudiness limited strong sun operation (Table 1). Moreover, Mat Su and Adamchuk (2023), observed that EC_a measurements done with Veris Quad EC 1000 (a set of contact electrodes), similar to MSP3, were relatively immune to long-term data drifts – soil conditions, and ambient temperatures. Despite the fact that it has been widely known that soil moisture at the time of EC_a survey affects EC_a values, few papers provide more exact information on the effect of this soil characteristic on EC_a values in non-saline soils. Brevik et al. (2006) observed at four of the five sites a linear relationship of EC_a (measured indirectly by EMI) with volumetric soil water content of fine-loamy soil samples collected in 0.15 m intervals to a depth of 0.9 m. The

Table 3
Descriptive statistics of absolute raw shallow (EC_{sh}) and deep (EC_{dp}) soil electrical conductivity data, respectively for eight and seven soil surveys

Sampling Year		Min	Max	Mean	Std	CV
2013	EC_{sh} (mS m^{-1})	0.39	9.42	2.02	1.33	65.9
2014		0.39	12.3	2.60	1.56	60.1
2015		0.65	15.9	3.12	1.57	50.2
2016		0.73	8.17	2.42	1.16	48.0
2017		0.58	9.91	2.84	1.53	53.9
2018		0.67	9.67	2.52	1.38	55.0
2019		1.61	12.6	4.52	1.77	39.1
2023		0.59	15.9	3.04	1.55	51.0
2013	EC_{dp} (mS m^{-1})	0.01	11.5	3.03	1.95	64.4
2014		–*	–	–	–	–
2015		0.80	11.7	2.46	1.2	48.6
2016		0.61	12.7	3.26	1.82	55.9
2017		0.53	13.0	3.43	2.02	59.0
2018		0.83	11.2	3.20	1.55	48.5
2019		1.93	13.3	5.40	1.68	31.0
2023		0.80	11.7	2.44	1.18	48.2

* – the EC_{dp} was measured, but the whole set of data contained quite a large amount of spurious (negative) EC_a values; therefore, it was not used for further processing

authors found out that EC_a has its greatest potential to differentiate between soils when the soils are moist. McCutcheon et al. (2006), measured EC_a of mainly loamy soils in semi-arid eastern Colorado using Veris 3100 equipment and found higher correlations (higher *r* values) of EC_a with volumetric soil water content (0.37–0.76), than with other soil properties, including soil separates. It was concluded that in dryland conditions, the EC_a measurements had limited utility for delineation of EC_a maps for variable rate application, but offer a potential method of mapping the relative spatial patterns of soil water content. According to the study done by Smagin (2006) in a laboratory on soil solution separated by centrifugation, the relationship between soil moisture and EC of soil solution was curvilinear. Maximum value of EC was obtained for soil moisture of 13% for light loams (according to Russian classification of ST), and 16%, and 18% for medium loams and heavy loams, respectively. In this study, soil moisture contents were probably calculated on mass basis. The averaged across all years, coefficient of variance of the absolute raw EC values was 52.9% and 50.8% for the shallow and deep EC_a measurements, respectively (unpresented data). The lowest and the highest variability for both – EC_{sh} and EC_{dp} values was registered at the same EC surveys, i.e. March 2019 and November 2013, respectively (Table 3). The high CV values of EC_a also indicate the high spatial variability of this soil property, which is necessary to develop MZs to vary the doses of agricultural inputs. In general, EC_a measured at both depths showed very similar spatial variability (CV values) when comparing results from the same EC survey. This is in contrast to the observations of Farahani and Buchleiter (2004), who found EC_{dp} to be more temporally stable than the corresponding EC_{sh}, even though major part of their fields had similar sandy and loamy sandy ST to our study. However, the study of Farahani and Buchleiter (2004) was conducted on pivot-irrigated fields, and this could have caused greater soil moisture changes in shallow soil layers than in the subsoil when compared to our rain-fed field.

3.3. Variation of interpolated (10 m x 10 m grid), EC_{sh} and EC_{dp} values with a field at subsequent EC surveys

As given in table 4, whole-field mean EC_a values showed variations over 10 years, ranging from 1.89 to 4.45 mS m^{-1} for shallow and from 2.40 to 5.07 mS m^{-1} for deep EC_a measurements. Since the interpolated EC_a values are generated using the absolute EC values, the former exhibited the same trends of variations as the original EC_a data. However, the range of both shallow and deep EC_a values was always, as expected, narrower for the interpolated EC_a values than for the original EC_a values.

The parameters (nugget, sill, and range) of the spherical semivariograms were, for the majority of the EC_a surveys, similar (Table 3s, supplementary materials). The main differences are visible for EC_a measurements done in 2015 and 2019, when the range of the variograms was shorter in comparison to the other years, indicating higher EC_a variability over shorter distances. At and beyond these distances, the EC_a values were not related.

Table 4
Descriptive statistics of interpolated shallow (EC_{sh}) and deep (EC_{dp}) soil electrical conductivity data, respectively for eight and seven soil surveys

Sampling Year		Min	Max	Mean	Std	CV
2013	EC_{sh} (mS m^{-1})	0.45	4.93	1.89	1.02	54.0
2014		0.51	6.30	2.49	1.33	53.4
2015		0.96	6.60	3.04	1.25	41.1
2016		0.86	5.04	2.39	0.98	41.2
2017		0.65	6.26	2.76	1.29	46.8
2018		0.74	5.75	2.47	1.17	47.3
2019		1.80	8.45	4.45	1.40	31.4
2023		0.87	7.08	3.18	1.34	42.0
2013	EC_{dp} (mS m^{-1})	0.48	7.34	2.84	1.63	57.4
2014		–*	–	–	–	–
2015		0.93	5.15	2.41	0.97	40.4
2016		0.79	6.90	3.20	1.51	47.2
2017		0.68	7.96	3.30	1.64	49.9
2018		0.91	6.81	3.07	1.31	42.7
2019		1.96	9.11	5.07	1.43	28.2
2023		0.93	5.07	2.40	0.97	40.2

* – the EC_{dp} was measured, but the whole set of data contained quite a large amount of spurious (negative) EC_a values; therefore, it was not used for further processing

The values of the nugget effect, which refers to the short-scale variability of EC_a (at distances smaller than the measurement intervals), were low and accounted for only 5.31–19.8% and 9.18–20% of the sill values for EC_{sh} and EC_{dp} (data not presented), respectively. Sill value reflects the maximum EC_a variability between points when they are far apart. However, the values of the nugget effect and sill in 2015 and 2019 were not specific and do not seem to be related to the amount of precipitation before the EC_a survey, because this was the highest in the above period in 2016, 2017, and 2018 (Table 1s, supplementary materials).

3.4. Relationship between interpolated EC_a values measured at different dates

The interpolated EC_a data derived for a 10 x 10 m grid were used to evaluate the variability of EC values across measurement days. The values of the correlation coefficients are given in Table 5 for EC_{sh} and in Table 6 for EC_{dp} data.

The correlations were generally high and very similar for both depths of EC_a measurements. The lowest correlations were obtained for EC_{sh} values measured in October 2015 and EC_{sh}

Table 5
Pearson correlation coefficients for shallow soil electrical conductivity (EC_{sh}) data

	EC_{sh}							
	2013	2014	2015	2016	2017	2018	2019	2023
2013	1.00							
2014	0.92	1.00						
2015	0.79	0.75	1.00					
2016	0.96	0.92	0.76	1.00				
2017	0.90	0.86	0.67	0.93	1.00			
2018	0.95	0.91	0.75	0.96	0.93	1.00		
2019	0.84	0.84	0.67	0.86	0.84	0.86	1.00	
2023	0.92	0.87	0.68	0.94	0.95	0.94	0.85	1.00

* – a critical value of r=0.067 at α=0.05, n=863

Table 6
Pearson correlation coefficients for deep soil electrical conductivity (EC_{dp}) data

	EC_{dp}						
	2013	2015	2016	2017	2018	2019	2023
2013	1.00						
2015	0.86	1.00					
2016	0.96	0.84	1.00				
2017	0.92	0.78	0.94	1.00			
2018	0.95	0.85	0.94	0.94	1.00		
2019	0.85	0.73	0.83	0.84	0.87	1.00	
2023	0.86	1.00	0.84	0.79	0.85	0.74	1

* – a critical value of r=0.067 at α=0.05, n=863

values registered during the other EC_a surveys. The same was not fully confirmed for EC_{dp} measured in 2015 as EC_{dp} values obtained at that time showed even perfect correlation (r=0.998) with EC_{dp} values obtained in October 2023.

These high correlations between EC_a values registered at both depths and across different years suggest that patterns of EC_a low, medium, and high values could be very similar and independent of measurement time. Similar observations were reported by Farahani and Buchleiter (2004), for EC_{dp} measurements performed on two mainly sandy fields and one loamy field in eastern Colorado, and one more loamy field (average clay content – 32%) located in SW Spain (Terrón et al., 2013; Terrón López, 2013) using the same Veris 3100 equipment both in Colorado and Spain. Out of the studies on temporal EC_a stability done with a non-contact EMI, high correlation values (from 0.78 to 0.96), between EC_a measurements performed at different dates were reported by De Caires et al. (2014).

3.5. Spatial (within a field) and temporal (across years) variability of relative EC_{sh} values

Figures 2 and 3 show the ranges of low (zero to 1), medium (from 1 to 2), and high (greather than 3) relative ECsh and ECdp values, across all measurement dates. An analysis of the distribution of relative EC_a values within the field for a single EC_a survey, allows for evaluating the within field EC_a variability. A comparison of this variability across EC_a measurement dates permits the evaluation of how relative EC values for a particular part of the field change from one EC_a survey to another.

Independently of the EC_{sh} measurement date, a significant part of the field (from 55.4 to 62.8%, data not presented) was characterized by relative EC_{sh} values equal to or lower than the whole-field average EC_{sh} over the eight EC_a measurements. Between 29.2 and 44.6% of the field area showed relative EC_{sh} values in the range of 1 and 2. A very small field area (between 0

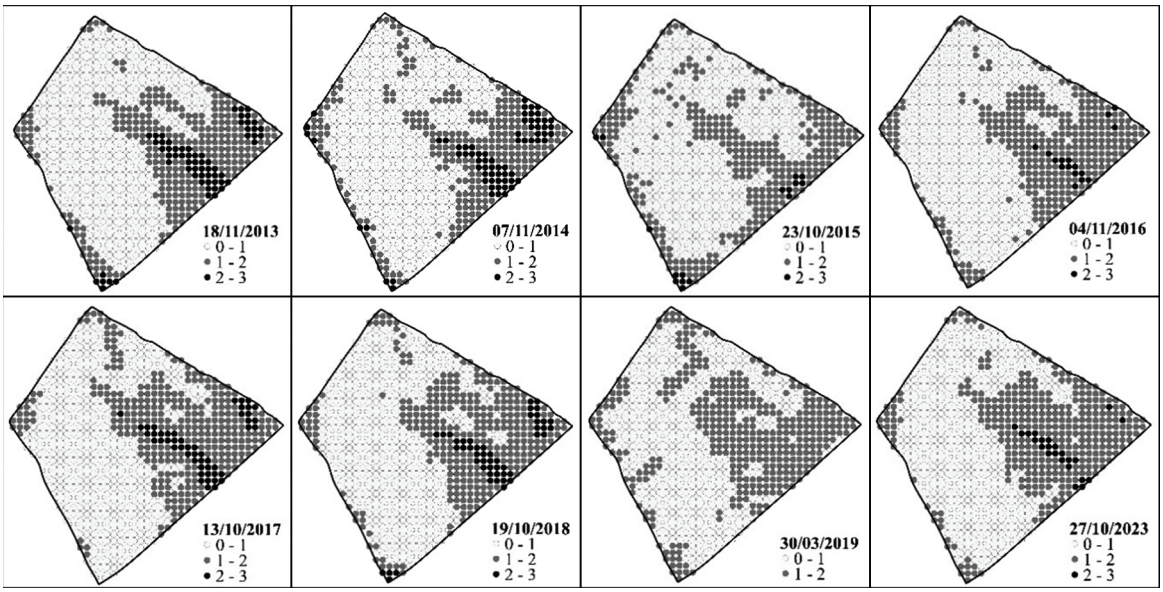

Fig. 2. Spatial (within a field) and temporal (across years) variability of relative EC_{sh} values registered during eight EC_a surveys from 2013 to 2023. The exact dates of the EC_a surveys are given next to each map

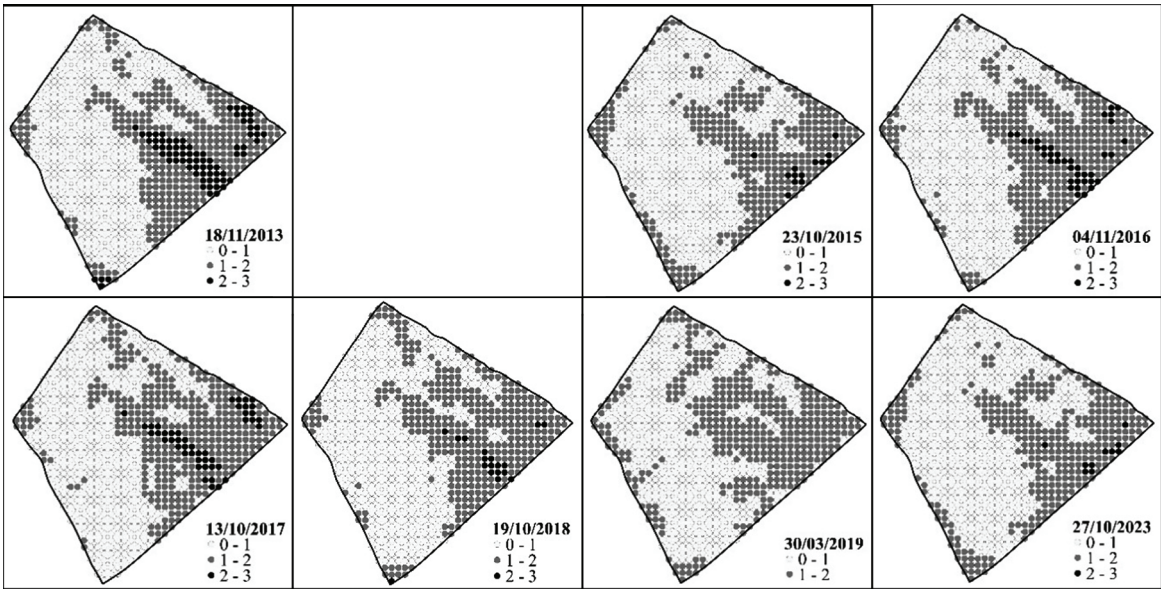

Fig. 3. Spatial (within a field) and temporal (across years) variability of relative EC_{dp} values registered during seven EC_a surveys from 2013 to 2023. The exact dates of the EC_a surveys are given next to each map

and 8.0%) was covered by relative EC_{sh} values above 2. In March 2019 the field was characterized by the lowest spatial EC_{sh} variation (Table 3). Therefore, the spatial variability of relative EC_{sh} values was also the lowest during this EC survey.

3.6. Spatial (within a field) and temporal (across years) variability of relative EC_{dp} values

Very similar patterns of relative EC_{dp} values were observed in subsequent EC_{dp} surveys (Fig. 3), as well as when comparing the distribution of relative EC_{sh} and EC_{dp} values within the field on the same measurement date (Fig. 2 and 3). Similar to the EC_{sh} measurements, the majority of the field (from 54.9 to 61.5%, data not presented) was characterized by relative EC_{dp} values that were lower than or equal to the whole-field average EC_{dp}. This is because the deeper EC_a measurement integrates over the entire 0–90 cm layer, and is influenced by properties in the top 30 cm (Veris Technologies, Pub. #AN 1CM02-5).

Relative EC_{dp} values between 1 and 2 covered 34.5 to 45.1% of the field area over the seven EC_{dp} measurements. And a very small part of the field (from 0 to 8,69%), was covered by relative EC_{dp} values above 2. These areas of the field could be characterized by finer ST and may require a different management. A previous study performed in the same field produced very similar patterns of ST, when this property was also indirectly assessed using the non-contact EMI method (Stępień et al., 2015). In other studies, similar spatial patterns for soil EC_a measurements done across different dates were obtained by Terrón López (2013) and Nyéki et al. (2022), who also used a contact method for EC_a measurements and by De Caires (2014), Liao et al. (2014), Serrano et al. (2017) and Badewa et al. (2019), who applied a non-contact EMI method. Serrano et al. (2024) obtained moderate correlation coefficients (from 0.449 to 0.618) between EC_a measurements done almost two years apart using the contact method and the EMI method.

3.7. Temporal variability of relative EC_{sh} and EC_{dp} values

After the evaluation of the EC_a variability over the years (expressed by CV values), the whole field area was divided into four classes of EC_a temporal variability, originally proposed by Pimentel-Gomes (2023). The following percentage of shallow relative EC_a values show CV values of below 10% – 10.08 (class 1), in the range of 10–20% – 65.93 (class 2), in the range of 20–30% – 19.35 (class 3) and above 30% – 4.64 (class 4); (Fig. 4a). In the case of the deep relative EC_a values, 16.34% (class 1) had CV below 10%, 54.35% (class 2) had CV in the range of 10–20%, 19.70% (class 3) had CV in the range of 20–30%, and 9.61% (class 4) was characterized by CV above 30% (Fig. 4b). In general, a significant part of the field (in total about 76% of EC_{sh} values and 70% of EC_{dp} values) was characterized by temporal stability because the CV value was below 20%. Similarly, to the results obtained by Farahani and Buchleiter (2004), who also used the contact method for EC_a measurements, we conclude that a single survey of this soil property should thus suffice to define stable zones without a need for remapping of non-saline and sandy soil. Otherwise, a lack of temporal stability in EC_a maps would dictate a need for repeated mappings that increase cost and complicate management (Farahani and Buchleiter, 2004).

Out of the 863 points, 57.8% did not change the CV class when comparing the temporal variability of the EC_{sh} and EC_{dp} measurements (Fig. 4c). No class change means that a particular point belonged to the same CV class range for example, 10–20% at both soil depths. Thirty-nine percent of the points changed the CV class by one class, and 3.13% changed the CV class by two classes. The results of the CV class comparison across the two soil depths indicate that soil EC_a on a significant part of this field shows similar temporal changes at both soil layers.

Farahani and Buchleiter (2004) performed a detailed analysis of the percent matching between individual EC_a delineations

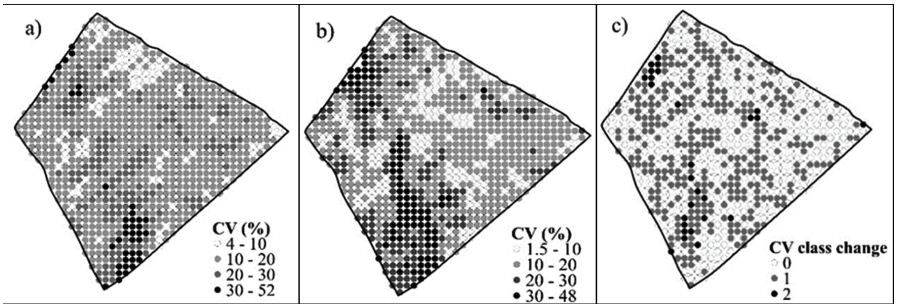

Fig. 4. Temporal variability (coefficient of variance, %) of relative: a) EC_{sh} values over eight years and b) EC_{dp} values over seven years and c) change of CV class for the above relative EC_a values. Consequently, null means no class change, 1 – change by one CV class, 2 – change by two CV classes

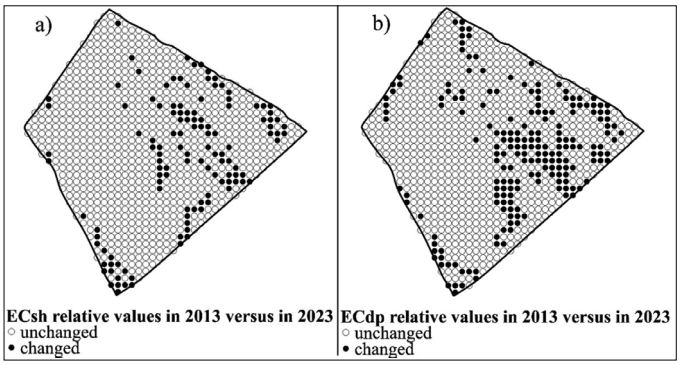

Fig. 5. Maps of stability of relative EC_a values (classes) over 10-year time: a) EC_{sh}, b) EC_{dp}

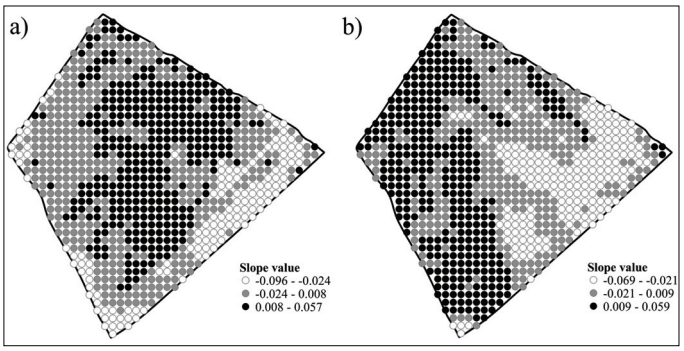

Fig. 6. Spatial variability of slope values of the regression line, used to indicate the rate of change of EC_a value over eight and seven years, respectively, for: a) EC_{sh}, and b) EC_{dp}

of low, medium, and high for all combinations of EC_a maps, i.e. coming from different EC_a measurement dates. This approach is only possible for scientific purposes, but a farmer interested in using an EC_a survey for MZ delineation will have these measurements usually done once in many years, as frequent EC_a surveys are not cost-effective. In this study, we follow the farmer's approach to some extent, namely assuming that crop rotation and field management after ten years might have affected the spatial EC_a patterns. Thus, we analyzed the matching of just two EC_a maps done in 2013 and 2023. In the case of the EC_{sh} and EC_{dp} relative values, only 14.4% and 22.6% (data not presented) of points changed the class of the relative EC_a values after this time interval, respectively (Fig. 5a and 5b). Therefore, due to the small changes described above, we entitled these figures as maps of stability of relative EC_a values but not maps of variability of relative EC_a values.

3.8. Identification of long-term trends of EC_a value changes

The time series analysis allowed us to detect patterns of change in EC_a values over the years. Generally, the slope values of the regression line, used to indicate the rate of change of EC_a value over the years, were low and very close to zero (Fig. 6a and 6b). Thus, these slight changes in EC_a values over the years could only indicate tendencies of this change. A positive slope value means that in these areas of the field, both EC_{sh} and EC_{dp} values increased over the years of EC_a measurements, while a negative slope means the opposite. The patterns of change in EC_a values over the years are different for EC_{sh} and EC_{dp} values.

3.9. Relationship between EC_{sh} and EC_{dp} measured in 2013 or 2023, and ST and fine particles determined in 2014

Consequently, following the farmer's approach described in the above section, the relationships between EC_a data registered only in 2013 and 2023 and soil separates determined in 2014 were evaluated. In both years the relationship between EC_a measured at 30 cm, and sand, silt, and clay content was very strong, moderately strong, and medium, respectively (Table 7). In both years, the relationships between EC_a measured at 90 cm, and sand, silt, and clay content were medium and, very similar in both years for all soil separates. In contrast, McCutcheon et al. (2006), who measured EC_a on four dates for mainly loamy soils, found low correlations (*r* values), between EC_a and clay (0.01–0.34), silt (0.05–0.32), and sand contents (between –0.36 and –0.04).

The results of PCA showed that the first two components explained between 93.7% and 96.4% of the variation of the soil data set (Fig. 7a–d). The patterns of correlations between EC_a measured at the same depth and all soil separates were very consistent in 2013 and 2023. A stronger negative impact of sand content on EC_a values was observed at the shallower layer than in the deeper layer. The EC_{sh} values were correlated with silt and clay content to a similar extent in 2013 and 2023. But, the EC_{dp} values correlated stronger with clay content than with silt content.

Table 7
The determination coefficients (R^2) of the best-fitted polynomial functions between interpolated and then normalized shallow and deep soil electrical conductivity measured in November 2013 or in October 2023 and soil separates, including fine particles determined in 2014

	Soil layer	Sand (0.05–2 mm)	Silt (0.002–0.05 mm)	Clay (<0.002 mm)	Fine particles (<0.02 mm)
			2013		
ECa_{sh}	0–30 cm	0.80	0.72	0.47	0.80
ECa_{dp}	0–90 cm	0.73	0.66	0.70	0.75
			2023		
ECa_{sh}	0–30 cm	0.76	0.65	0.50	0.76
ECa_{dp}	0–90 cm	0.71	0.64	0.69	0.71

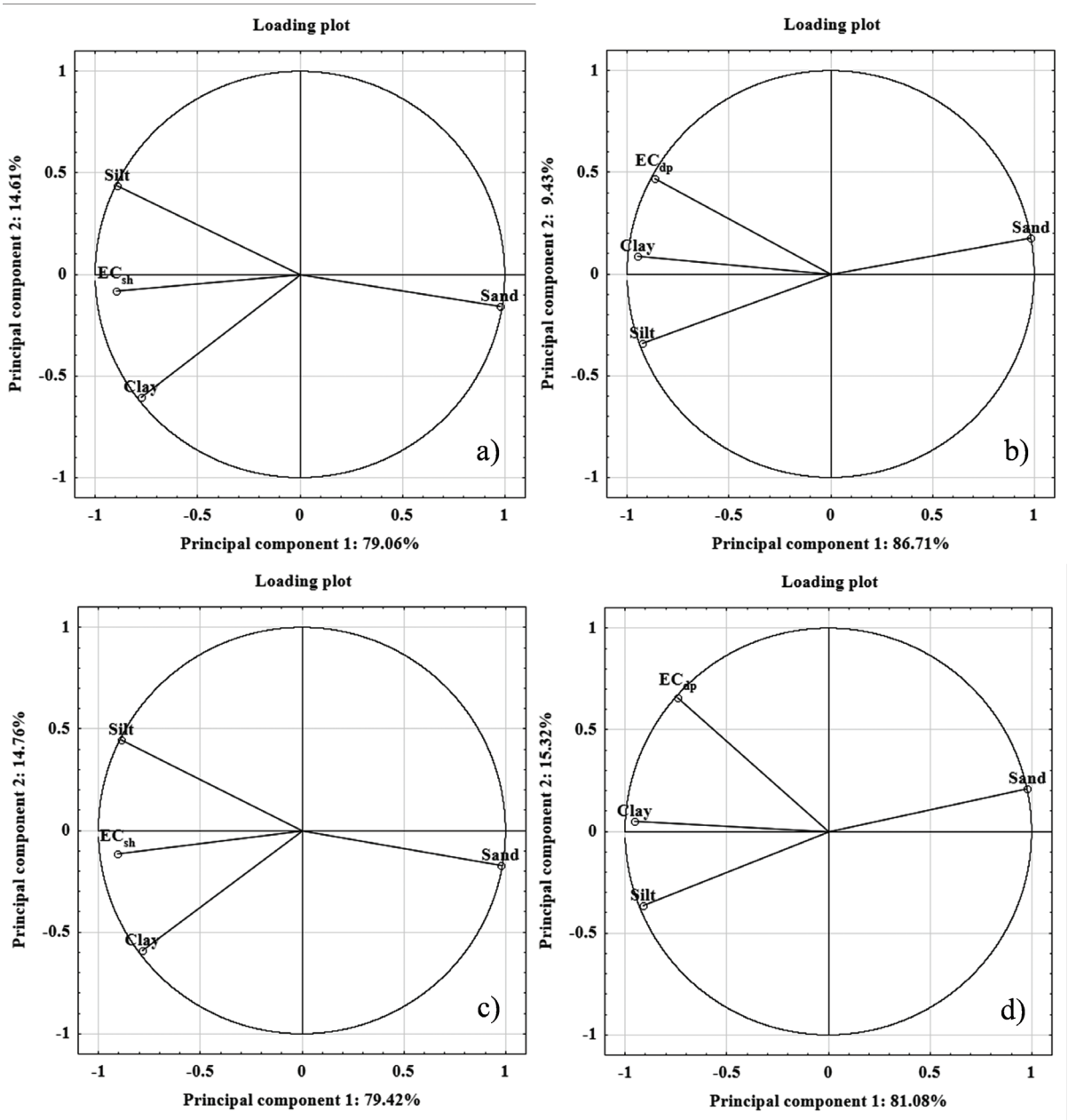

Fig. 7. Principal component analysis graphs explaining the impact of soil separates on EC_a values: a) EC_{sh} in 2013, b) EC_{dp} in 2013, c) EC_{sh} in 2023, and d) EC_{dp} in 2023

In our study, FPs content in both years was strongly related to EC_{sh} and EC_{dp}, using a second-order polynomial regression, with R^2 values of 0.80 and 0.75 in 2013 and R^2 values of 0.76 and 0.71 in 2023, respectively in the shallow and deeper soil layer (Table 7). In the previous studies carried out in Poland by Stępień et al. (2015, 2017), a negative correlation between EC_a and sand content, and a positive correlation between EC_a and FPs, silt, and clay was observed.

The high R^2 values indicate that the EC_a patterns are mainly attributed to soil separates in non-saline and sandy soils. Thus, on such type of soils, ground-truth soil samples should be collected to calibrate EC_a to the soil separates, which mainly influence EC_a (Corwin and Scudiero, 2020). Since 1986 the ACs have been used in Poland for formulating fertilizer recommendations (Zalecenia nawozowe, 1990; Jadczyszyn et al., 2010; Jadczyszyn et al., 2016). These categories are derived using the information on soil separates determined directly by means of a laboratory (pipette and hydrometer), method, or the texture by feel test. Because we found strong and significant correlations between the content of FPs, and EC_a measured at both depths (Table 7, Fig. 8a, 8b, 9a, and 9b), an approach that allows for determining ACs directly using the relative values of EC_a measurements is proposed. The MAE of the predicted FPs content using relative values of EC_a from 2013 was 1.87 and 4.38 for EC_{sh} and EC_{dp} measurements (Fig. 8a and 9a), respectively.

In 2023 the MAE value was 2.02 and 4.54 for EC_a measurements done at the same layers as above (Fig. 8b and 9b). The relationships between FP (%) and relative EC_{sh} and EC_{dp} values, expressed by the quadratic models from figures 8a and 8b, and 9a and 9b were used to recalculate the relative EC_{sh} and EC_{dp} values to the percent of FPs and create maps of soil ACs (Fig. 10a, 10b, 11a and 11b).

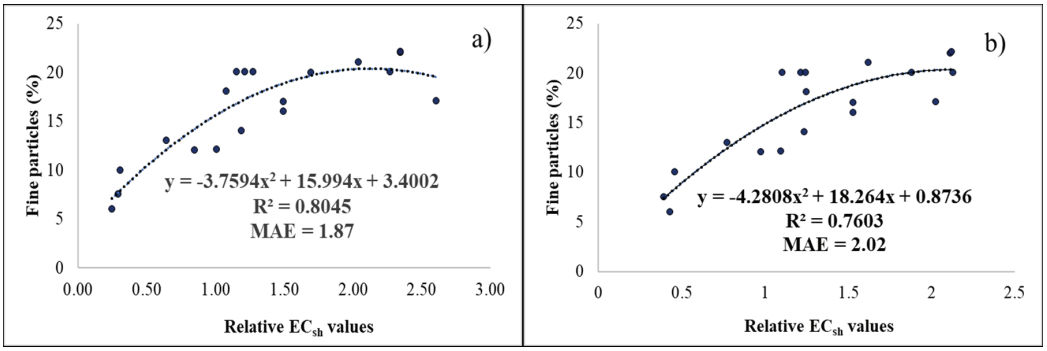

Fig. 8. Relationship between relative EC_{sh} values measured in: a) November 2013 and b) October 2023, and fine soil particles (%) determined in 2014, and mean absolute error of the predicted fine particles content

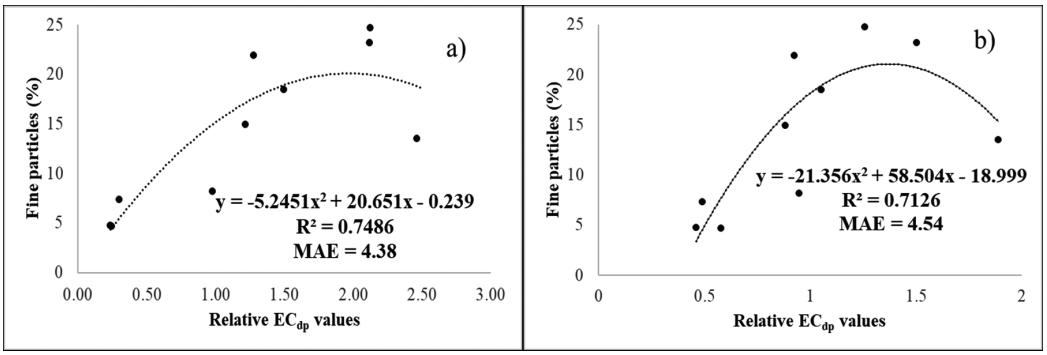

Fig. 9. Relationship between relative EC_{dp} values measured in: a) November 2013 and b) October 2023 and fine soil particles (%) determined in 2014, and mean absolute error of the predicted fine particles content

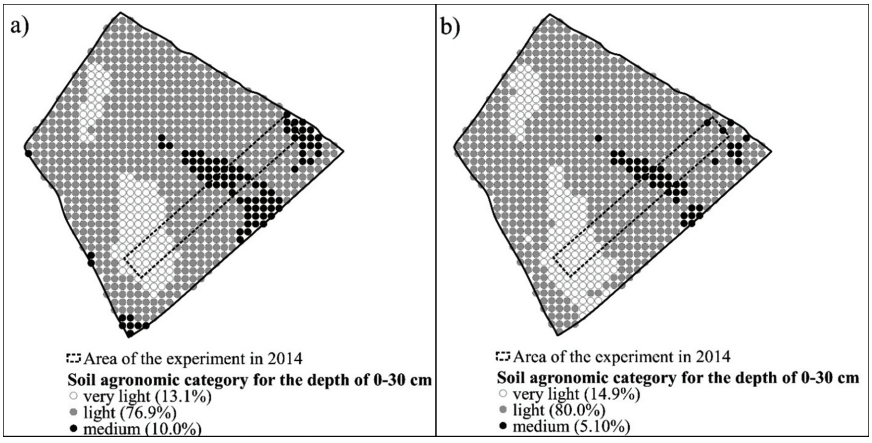

Fig. 10. Map showing the precentage of soil agronomic categories to a depth of 0–30 cm, when the relative EC_{sh} values from: a) November of 2013 and b) October of 2023 were used to predict the fine particles content, with the experimental area of 0.90 ha in 2014, superimposed

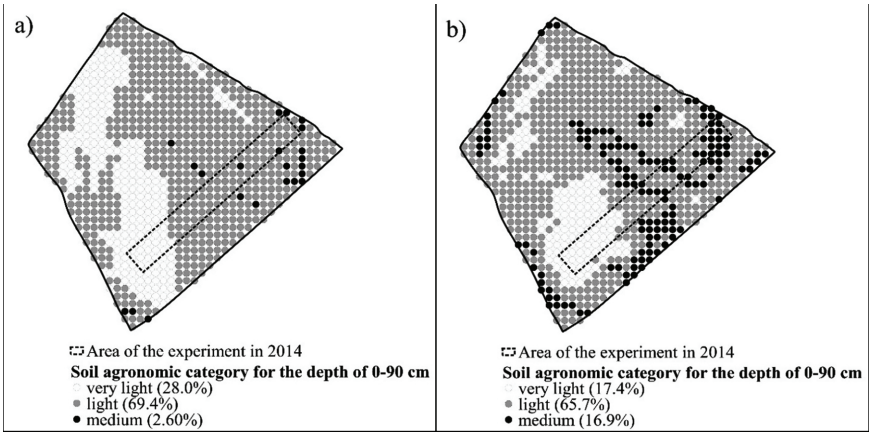

Fig. 11. Map showing the precentage of soil agronomic categories to a depth of 0–90 cm, when the relative EC_{dp} values from: a) November of 2013 and b) October of 2023 were used to predict the fine particles content, with the experimental area of 0.90 ha in 2014, superimposed

3.10. Maps of soil agronomic categories based on predicted FPs content using relative EC_{sh} and EC_{dp} values

It was observed that when using EC_{sh} data from both years for the creation of ACs a significant part (76.9% in 2013, and 80.0% in 2023) of the field area was covered by light soils in the shallow layer of 30 cm; the remaining part of the field was covered by very light soil (13.1% in 2013 and 14.9% in 2023), and medium soil (10.0% in 2013 and 5.10% in 2023), figures 10a and 10b.

The areas of these three ACs occur, independently of the year from which the EC_a data were used, in well-defined and relatively extensive areas that can be sampled separately to determine accurately liming needs and K and Mg availability in soil (Zalecenia nawozowe, 1990) and then use these results for the variable application of lime, potassium, and magnesium fertilizers (Stępień and Samborski, 2018) which are recommended mainly on the base of ACs (lime and K, Mg fertilizers) and expected yields (K fertilizers).

In the layer of 90 cm, the soil was more variable and consisted of three ACs: very light (28.0%), light (69.4%), and medium (2.60%) soils, when EC_a relative data from 2013 were used for the creation of the ACs maps. When the relative EC_{dp} data from 2023 were used for the delineation of ACs maps, a higher area of medium soils (16.9%) and a lower area of very light soils (17.4%) were calculated in comparison when EC_{dp} data from 2013 were applied (Fig. 11a and 11b). However, when the EC_{dp} data from 2013 were used, medium soils occurred in very small areas and in 2023 the latter AC, occurred in greater but most frequently long and narrow areas scattered over the field, that are rather difficult to be considered during the variable application of fertilizers. On the contrary, main areas of very light and light soils might be delineated much more easily on this field, independently of the year from which the EC_a data were used, and thus considered in the application of variable input (N, P and K fertilizers, seeds) rates, which doses are based in a great part on expected yields (Stępień and Samborski, 2018). Crop yields depend not only on the ST of the topsoil but also on the ST of deeper layers that could be indirectly determined by measuring EC_{dp}. Moreover, the information soil AC for layers 0–30 cm and 30–60 cm is taken into account when the amount of mineral nitrogen (N_{min}) in very early spring is calculated using the methodology developed by Fotyma et al. (1998) and described in fertilizer recommendations for Polish farmers by Jadczyszyn et al. (2010). The AC of heavy soils (FP content above 35%) does not appear on the investigated field. However, some layers of heavy soils were detected in small areas of the field during soil sampling, but after calculation of the averaged contents of FPs to a depth of 90 cm, the areas of heavy soils were not delineated within the field. In general, the AC maps delineated using the EC_{sh} obtained in 2013 and 2023 look very similar. Less consistency of the ACs maps could be observed when the EC_{dp} data were used for their delineation and compared for 2013 and 2023. The differences in the ACs maps (Fig. 11a and 11b), are due to different patterns of the relative EC_{dp} values in 2013 and 2023 (Fig. 3), and various shapes of the polynomial functions in figures 9a and 9b used to calibrate the EC_{dp} values against FPs. The latter differences were caused because some out of the ten soil samples used for the calibration were assigned significantly different relative EC_{dp} values in 2013 and 2023. The use of relative EC_a values calculated using the absolute EC_a values and soil sampling to determine soil separates, including FPs content, exactly at the points when the ECa was registered with the use of GNSS-RTK receiver can increase the EC_a values calibration accuracy. Since our relationship between the content of FPs and EC_a readings was limited to a set of these particular field conditions, wider applications of calibration relations or models, as suggested by Adamchuk et al. (2021), might not always be appropriate, because soil predictions are site-specific and, according to our results, even date-specific (Fig. 8 and 9). Our previous research results show that the relationships between the content of sand, silt, clay and EC_a values are field-specific and produce different regression equations, which could be applied for ST or AC delineation on the field (Stępień et al., 2015; Stępień et al., 2017; Stępień and Samborski, 2018). For this reason, we suggest using the same set of soil samples of various ST taken once to calibrate EC_a measurements across years, separately for each field and each EC_a survey. Unless the fields for which ECa calibration is going to be done are of similar ST, and status at the time of ECa mapping, e.g. stubble. Then the same set of soil samples can be used to calibrate ECa data for more fields.

The number of soil samples used for EC_a calibration should be reduced in comparison to our study, but still representative for a particular field, to make this method applicable to farm

conditions (Stępień and Samborski, 2018). On the other hand, the use of the PSS offers growers and their advisers also tools which help assessing where to take soil samples (GRDC 2023).

4. Conclusions

1. The production field was characterized by high spatial variability of EC_{sh} and EC_{dp} values during each of the EC_a measurements and also by stable patterns compared over eight and seven EC_a surveys, respectively. This means that a single EC_{sh} and EC_{dp} measurement should be sufficient to delineate maps of soil physical properties strongly related to soil electrical conductivity such as ST in non-saline and sandy soils.
2. A strong relationship between the relative EC_{sh} and EC_{dp} values and fine soil particles (<0.02 mm) allowed the creation of maps of soil ACs in non-saline and sandy soils. The patterns of soil ACs were repeatable across years (2013 vs. 2023), but more acceptable for map generalization when the EC_{sh} values were used to predict FPs content. However, a wider application of these relationships for formulating fertilizer recommendations may require field-specific calibrations to ensure AC delineation accuracy.

Acknowledgments

The authors thank the management of the experimental farm of Warsaw University of Life Sciences in Obory for their technical support and for allowing us to undertake the study on their field. We fully acknowledge: Dr hab. Dariusz Gozdowski, Dr inż. Elżbieta Bodecka, Dr inż. Joanna Groszyk, Dr hab. Marcin Studnicki, and M. Sc. students for their help with soil sampling and texture determination. The part of the research related to soil sampling and ST analysis was supported by a scientific project POIG.01.03.01-14-041/12 – "BIOPRODUCTS, innovative technologies of pro-health bakery products and pasta with reduced caloric value" co-financed by the European Regional Development Fund under the Innovative Economy Operational Programme in the years 2007–2013. The authors also thank Prof. dr hab. Jan Rozbicki for the management of this project.

Conflict of interest

The authors declare no conflict of interest and that they have no known competing financial interests or personal relationships that could have appeared to influence the work reported in this paper. This research did not involve human or animal subjects.

Author Contributions

Stanisław Marek Samborski – Conceptualization, Data curation, Investigation, Methodology, Supervision, Validation, Writing – original draft. **Michał Stępień** – Conceptualization, Investigation, Methodology, Writing – review & editing. **Yunus Emre Şekerli** – Visualization, Investigation, Writing – review & editing. All authors read and approved the final manuscript.

References

Adamchuk, V. et al., 2021. [In:] Kerry, R., Escolŕ, A. (Eds.), Sensing approaches for precision agriculture. Progress in Precision Agriculture. Springer, Cham, 93–132. https://doi.org/10.1007/978-3-030-78431-7_4

Adamchuk, V.I., Rossel, R.A.V., Sudduth, K.A., Lammers, P.S., 2011. Sensor fusion for precision agriculture. [In:] Thomas, C. (Ed.), Sensor Fusion – Foundation and Applications. Intech Open, 27–40. https://doi.org/0.5772/19983

Adamchuk, V.I., Hummel, J.W., Morgan, M.T., Upadhyaya, S.K., 2004. On-the-go soil sensors for precision agriculture. Computers and Electronics in Agriculture 44, 71–91. https://doi.org/10.1016/j.compag.2004.03.002

Ahrends, H.E., Simojoki, A., Lajunen, A., 2023. Spatial pattern consistency and repeatability of proximal soil sensor data for digital soil mapping. European Journal of Soil Science 74(5), e13409. https://doi.org/10.1111/ejss.13409

Atwell, M.A., Wuddivira, M.N., 2019. Electromagnetic-induction and spatial analysis for assessing variability in soil properties as a function of land use in tropical savanna ecosystems. SN Applied Sciences 1, 856. https://doi.org/10.1007/s42452-019-0902-9

Badewa, E., Unc, A., Cheema, M., Galagedar, L., 2019. Temporal stability of soil apparent electrical conductivity (ECa) in managed podzols. Acta Geophysica 67, 1107–1118. https://doi.org/10.1007/s11600-019-00306-1

Blackmore, S., 2000. The interpretation of trends from multiple yield maps. Computers and Electronics in Agriculture 26, 37–51. https://doi.org/10.1016/S0168-1699(99)00075-7

Bioprodukty, 2013–2015. Unpublished results obtained during the realization of scientific project POIG.01.03.01-14-041/12—"BIOPRODUCTS, innovative technologies of prohealth bakery products and pasta with reduced caloric value", co-financed by the European Regional Development Fund under the Innovative Economy Operational Programme 2007–2013.

BN, 1978. BN-78/9180-11. Gleby i utwory mineralne. Podział na frakcje i grupy granulometryczne. Norma branżowa.

Bohling, G., 2005. Introduction to geostatistics and variogram analysis. Available at: http://gismyanmar.org/geofocus/wpcontent/uploads/2013/01/Variograms.pdf

Bottega, E.L., Queiroz, D.M., Pinto, F.D., Souza, C.M., Valente, D.S., 2017. Precision agriculture applied to soybean: Part I – Delineation of management zones. Australian Journal of Crop Science 11, 573–579. https://doi.org/10.21475/ajcs.17.11.05.p381

Brevik, E.C., Fenton, T.E., Lazari, A., 2006. Soil electrical conductivity as a function of soil water content and implications for soil mapping. Precision Agriculture 7, 393–404. https://doi.org/10.1007/s11119-006-9021-x

Corwin, D.L., Scudiero, E., 2020. Field-scale apparent soil electrical conductivity. Soil Science of America Journal 84, 1405–1441. https://doi.org/10.1002/saj2.20153

Corwin, D.L., Lesch, S.M., 2003. Application of soil electrical conductivity to precision agriculture: theory, principles, and guidelines. Agronomy Journal 95, 455–471. https://doi.org/10.2134/agronj2003.4550

De Caires, S.A., Wuddivira, M.N., Bekele, I., 2014. Assessing the temporal stability of spatial patterns of soil apparent electrical conductivity using geophysical methods. International Agrophysics 28(4), 423–433. https://doi.org/10.2478/intag-2014-0033

de Farias, M.F. et al., 2018. Potassium fertilization in soybean and its correlation with electrical conductivity in soil. Journal of Agricultural Science 10(12), 336–343. https://doi.org/10.5539/jas.v10n12p336

Farahani, H.J., Buchleiter, G.W., 2004. Temporal stability of soil electrical conductivity in irrigated sandy fields in Colorado. Transactions of the American Society of Agricultural Engineers 47(1), 79–90. https://doi.org/10.13031/2013.15873

Fotyma, E., Wilkos, G., Pietruch, Cz., 1998. Test glebowy azotu mineralnego – możliwości praktycznego wykorzystania, Materiały Szkoleniowe IUNG, Puławy.

QGIS.org, 2022. QGIS Geographic Information System. Open Source Geospatial Foundation Project. http://qgis.org. Accessed 3 January 2025.

Gonçalves, L.A., de Souza, E.G., Nóbrega, L.H.P., Bier, V.A., Magii, M.F., Bazzi, C.L., Uribe-Opazo, M.A., 2025. Spatial and temporal variability of soil apparent electrical conductivity. Precision Agriculture 26, 10. https://doi.org/10.1007/s11119-024-10209-x

Grains Research and Development Corporation, 2023. An overview of the different proximal soil sensing systems available to Australian growers, and for use in precision agriculture. Proximal soil sensing systems. Fact Sheet. SPA2201-001SAX.

IUSS Working Group WRB, 2022. World Reference Base for Soil Resources. International soil classification system for naming soils and creating legends for soil maps 4th edition. International Union of Soil Sciences, IUSS, Vienna, Austria, 1–236.

Jadczyszyn, T., Kowalczyk, J., Lipiński, W., 2010. Zalecenia nawozowe dla roślin uprawy polowej i trwałych użytków zielonych. Materiały szkoleniowe Nr 95, IUNG Puławy.

Jadczyszyn, J., Niedźwiecki, J., Debaene, J., 2016. Analysis of agronomic categories in different soil texture classification systems. Polish Journal of Soil Science 20, 49–72. https://doi.org/10.17951/pjss/2016.49.1.61

Kabała, C. et al., 2019. Polish Soil Classification, 6th edition – principles, classification scheme and correlations. Soil Science Annual 70(2), 71–97. https://doi.org/10.2478/ssa-2019-0009

Liao, K.H., Zhu, Q., Doolittle, J., 2014. Temporal stability of apparent soil electrical conductivity measured by electromagnetic induction techniques. Journal of Mountain Science 11(1). https://doi.org/10.1007/s11629-012-2630-0

Łopatka, A., 2017. Europejski monitoring użytkowania gruntów i baza danych projektu LUCAS. Studia i Raporty IUNG-PIB 51(5), 73–89.

Lueck, E., 2015. The influence of fertilization on electrical conductivity data. First Conference on Proximal Sensing Supporting Precision Agriculture 1, 1–5. https://doi.org/10.3997/2214-4609.201413838

Mat Su, AS., Adamchuk, VI., 2023. Temporal and operation-induced instability of apparent soil electrical conductivity measurements. Frontiers in Soil Science. 3, 1137731. https://doi.org/10.3389/fsoil.2023.1137731

McCutcheon, M.C., Farahani, H.J., Stednick, J.D., Buchleiter, G.W., Green, T.R., 2006. Effect of soil water on apparent soil electrical conductivity and texture relationships in dryland field. Biosystems Engineering 94(1), 19–32. https://doi.org/10.1016/j.biosystemseng.2006.01.002

McKenzie, N., Bramley, R., Farmer, T., Janik, L., Murray, W., Smith, Ch., McLaughlin, M., 2003. Rapid soil measurement – a review of potential benefits and opportunities for the Australian grains industry. Report for the Grains Research and Development Corporation. pp. 41.

Molin, J.P., Faulin, G.D. Ch., 2013. Spatial and temporal variability of soil electrical conductivity related to soil moisture. Scientia Agricola 70(1), 1–5. https://doi.org/10.1590/S0103-90162013000100001

Nyéki, A., Daróczy, B., Kerepesi, C., Neményi, M., Kovács, A.J., 2022. Spatial variability of soil properties and its effect on maize yields within field – a case study in Hungary. Agronomy 12(2), 395. https://doi.org/10.3390/agronomy12020395

Pedrera-Parrilla, A., Brevik, E.C., Giráldez, J.V., Vanderlinden, K., 2016. Temporal stability of electrical conductivity in a sandy soil. International Agrophysics 30, 349–357. https://doi.org/10.1515/intag-2016-0005

Pierce, F.J., Nowak, P., 1999. Aspects of precision agriculture. Advances in Agronomy 67, 1–85. https://doi.org/10.1016/S0065-2113(08)60513-1

Pimentel-Gomes, F., 2023. Curso De estatística experimental. Digitaliza Conteúdo

Polskie Towarzystwo Gleboznawcze, 2009. Klasyfikacja uziarnienia gleb i utworów mineralnych – PTG 2008. Roczniki Gleboznawcze – Soil Science Annual 60 (2), 5–16.

Richling, A., 2021. Charakterystyka prowincji i podprowincji (Description of provinces and subprovinces). [In:] Richling, A., Solon, J., Macias, A., Balon, J., Borzyszkowski, J., Kistowski, M. (Eds.), Regionalna geografia fizyczna Polski. Bogucki Wyd. Naukowe, Poznań, 39–65.

Sarnacka, Z., 1976. Szczegółowa mapa geologiczna Polski 1:50 000. Arkusz 560 Piaseczno. PIG. Scan of the map was downloaded from CBDG (Central Geological Database): https://baza.pgi.gov.pl/resources.html?type=smgp&id=560

Serrano, J.M., Shahidian, S., Marques da Silva, J., 2017. Spatial variability and temporal stability of apparent soil electrical conductivity in a Mediterranean pasture. Precision Agriculture 18, 245–263. https://doi.org/10.1007/s11119-016-9460-y

Serrano, J., Shahidian, S., Silva, J.M., Paniágua, L.L., Rebollo, F.J., Moral, F.J., 2024. Temporal stability of management zone patterns: case study with contact and non-contact soil electrical conductivity sensors in dryland pastures. Sensors 24, 1623. https://doi.org/10.3390/s24051623

Smagin, A.V., 2006. Soil-hydrological constants: the physical meaning and quantification on the basis of equilibrium centrifugation. Interactive Journal of Ecological Soil Science 1, 1 (in Russian)

Solon, J., et al., 2018. Physico-geographical mesoregions of Poland: Verification and adjustment of boundaries on the basis of contemporary spatial data. Geographia Polonica 91(2), 143–170. https://doi.org/10.7163/GPol.0115

Stępień, M., Gozdowski, D., Bodecka, E., Groszyk, J., Rozbicki, R., Samborski, S., 2017. Topsoil texture maps based on calibration of soil electrical conductivity with soil datasets varying in size. Polish Journal of Soil Science 50(2), 265–278. https://doi.org/10.17951/pjss/2017.50.2.265

Stępień, M., Gozdowski, D., Samborski, S., 2024a. Możliwości przypisania zawartości frakcji granulometrycznych według PTG 2008/USDA do wybranych grup granulometrycznych PTG 1956 wyróżnionych na mapie glebowo-rolniczej. Soil Science Annual 75(3), 183375. https://doi.org/10.37501/soilsa/193375

Stępień, M., Gozdowski, D., Samborski, S., 2024b. How Accurately Is Topsoil Texture Shown on Agricultural Soil Maps? A Case Study of Eleven Fields Located in Poland. Land 13, 1852. https://doi.org/10.3390/land13111852

Stępień, M., Samborski, S., Gozdowski, D., Dobers, E.S., Chormański, J., Szatyłowicz, J., 2015. Assessment of soil texture class on agricultural fields using ECa, Amber NDVI, and topographic properties. Journal of Plant Nutrition and Soil Science 178(3), 523–536. https://doi.org/10.1002/jpln.201400570

Stępień, M., Samborski, S., 2018. Ocena właściwości gleby na potrzeby rolnictwa precyzyjnego [In:] Samborski, S. (Ed.). Rolnictwo precyzyjne. Wydawnictwo Naukowe PWN S.A., Warsaw, Poland, pp. 1–522. (in Polish)

Systematyka gleb Polski, 2019. Polskie Towarzystwo Gleboznawcze, Komisja Genezy, Klasyfikacji i Kartografii Gleb. Wydawnictwo Uniwersytetu Przyrodniczego we Wrocławiu, Polskie Towarzystwo Gleboznawcze, Wrocław–Warszawa, pp. 235.

Terrón López, J.M., 2013. Delimitación de zonas de manejo en agricultura de precisión a partir de medidas de conductividad eléctrica aparente del suelo mediante el uso de sensores móviles de contacto. PhD thesis, University of Córdoba. Available at: https://helvia.uco.es/handle/10396/10181.

Terrón, J., Moral, F., da Silva, J.M., Rebollo, F., 2013. Analysis of spatial pattern and temporal stability of soil apparent electrical conductivity and relationship with yield in a soil of high clay content. In 3rd Global Workshop on Proximal Soil Sensing, 302–306.

Veris Technologies. Pub. #AN 1CM02-5.

Witek, T., 1973. Mapy glebowo-rolnicze oraz kierunki ich wykorzystania. Instytut Uprawy, Nawożenia i Gleboznawstwa, Puławy. PWRiL, Warszawa, 75 ss. Available at: https://www.gov.pl/web/gugik/materialy-dotyczace-map-glebowo-rolniczych, Accessed 15 January 2025.

Zalecenia Nawozowe Cz. I. Liczby Graniczne do Wyceny Zawartości Makro-i Mikroelementów w Glebach, 2nd ed., 1990. Instytut Uprawy Nawożenia i Gleboznawstwa, Puławy, Poland, 1–28.

Zhu, Q., Lin, H., Doolittle, J., 2010. Repeated electromagnetic induction surveys for improved soil mapping in an agricultural landscape. Soil Science Society of America Journal 74(5), 1763–1774. https://doi.org/10.2136/sssaj2010.0056

Studium przypadku stabilności czasowej przewodności elektrycznej gleby, na polu o glebie piaszczystej oraz przydatność jej pomiaru do przygotowania map kategorii agronomicznych

Słowa kluczowe

Uziarnienie gleby
Kategoria agronomiczna
Gleba lekka i bardzo lekka
Pozorna przewodność elektryczna
Stabilność czasowa

Streszczenie

Jednym z najczęściej używanych sposobów oceny przestrzennej zmienności gleby jest pomiar pozornej przewodności elektrycznej gleby (ang. *apparent electrical conductivity* – EC_a), podczas przejazdu urządzenia z zamontowanym czujnikiem, po polu. Jeśli wartości EC_a zostaną poprawnie skalibrowane względem innych właściwości gleby ocenianych laboratoryjnie, pomiar EC_a gleby może pomóc stworzyć mapy glebowe, które przedstawiają zróżnicowanie tych właściwości. Następnie mapy te, po reklasyfikacji, mogą zostać użyte do stworzenia map stosowania zmiennej dawki środków produkcji, aby zwiększyć efektywność ich wykorzystania. Jeśli zasolenie gleby nie występuje, EC_a jest silnie zależna od uziarnienia gleby, które jest bardziej stabilne w czasie niż właściwości chemiczne gleby. Jednakże, stabilność wyników pomiarów EC_a w czasie nie była badana w Polsce, gdzie występują znaczne powierzchnie gleb bardzo lekkich i lekkich. W naszym kraju wyróżniono cztery kategorie agronomiczne gleb (KAG), wydzielane na podstawie zawartości części spławialnych (<0.02mm) w glebie. KAG wykorzystywane do formułowania zaleceń wapnowania i nawożenia, są zwykle wydzielane za pomocą laboratoryjnego określenia udziału części ziemistych lub odczytywane z map glebowo-rolniczych. Ale żaden z tych sposobów nie pozwala na wydzielanie KAG z dużą gęstością przestrzenną, wymaganą do wykonania map stosowania zmiennej dawki środków produkcji. Celem badań było: i) oszacowanie przestrzennej i czasowej zmienności względnych wartości EC_a zarejestrowanych na dwóch głębokościach (0–30 and 0–90 cm), w trakcie ośmiu pomiarów EC_a w obrębie pola produkcyjnego, gdzie dominują gleby bardzo lekkie i lekkie; ii) określenie KAG dla tego pola, w oparciu o zależności między wartościami EC_a, zarejestrowanymi podczas dwu pomiarów, które wykonano w 10-letnim odstępie czasu, a ilością części ziemistych. Wyniki badań wykazały, że pole produkcyjne charakteryzowało się dużą zmiennością przestrzenną EC_a i stabilnością czasową wydzielonych obszarów EC_a, co sugeruje że pojedynczy pomiar tej właściwości gleby może być wystarczający do wyrysowania map fizycznych właściwości gleby silnie związanych z EC_a na glebach bardzo lekkich i lekkich. Silna zależność między względnymi wartościami EC_a zarejestrowanymi 2013 i 2023 roku i zawartością części ziemistych pozwoliła na narysowanie bardzo podobnych map KAG, które mogą być wykorzystane do formułowania zaleceń wapnowania i nawożenia na ww. glebach. Układ KAG był mniej powtarzalny w latach (2013 i 2023), ale akceptowalny do celów generalizacji tych map, gdy do przewidywania zawartości części spławialnych wykorzystano dane EC z grubszej warstwy gleby (0–90 cm). Jednakże, szersze zastosowanie uzyskanych zależności może wymagać kalibracji danych EC_a dla danego pola, aby zapewnić lepszą dokładność wykonania map KAG, gdyż badania te zostały przeprowadzone na jednym polu produkcyjnym.